Phase behaviour of hydrogen-bonded liquid crystalline complexes of alkoxycinnamic acids with 4,4'-bipyridine

Yoon-Sok Kang; Heesub Kim; Wang-Cheol Zin

PLEASE SCROLL DOWN FOR ARTICLE

Phase behaviour of hydrogen-bonded liquid crystalline complexes of alkoxycinnamic acids with 4,4′-bipyridine

YOON-SOK KANG, HEESUB KIM and WANG-CHEOL ZIN*

Department of Materials Science and Engineering and Polymer Research Institute,
Pohang University of Science and Technology, Pohang 790-784, Korea

The hydrogen-bonded liquid crystalline complexes of 4-*n*-alkoxycinnamic acids (*n*CNA: *n* = 4–8, 10, 12, 16, 18, where *n* is the number of carbons in the alkoxy chain) with 4,4′-bipyridine (BPy) have been prepared and characterized. The existence of smectic C, smectic A, and nematic mesophases of these complexes was demonstrated by a combination of polarized optical microscopy and X-ray diffraction (XRD). In this H-bonded mesogenic structure, non-mesogenic BPy functions as the core unit of the mesogen through the H-bond, as confirmed by infrared spectroscopy and XRD. A general comparison of *n*CNABPy with the benzoic acid analogues (*n*OBA)$_2$-BPy, showed that the elongated *n*CNABPy mesogen behaves as a rod unit and increases the transition temperature. Smectic phases in *n*CNAs ($5 \leqslant n \leqslant 12$) were induced on complexation with BPy. The favouring of smectic phases in these complexes is believed to originate from the increment of polarity of the mesogen by intermolecular H-bonding. With increasing chain length of the *n*CNABPy complexes the smectic C phase becomes stabilized, like conventional rod–coil molecules.

1. Introduction

The development of supramolecular chemistry involves the control of molecular interactions to yield well defined materials; the formation of supramolecular structures using small molecular components is of great chemical and biological interest [1]. In liquid crystals, mesomorphism results from a proper combination of molecular interactions and the shape of molecules. A conventional low molar mass liquid crystal comprises molecules consisting of a semi-rigid anisometric core attached normally to one or two alkyl chains [2]. It is the anisotropic interactions between the cores that give rise to liquid crystalline behaviour, while the role of the alkyl chains is largely to reduce the transition temperatures of the material. In these molecules, the mesogenic core often contains phenyl rings connected via short unsaturated linkages. In recent years, however, increasing research has focused on materials in which the core is assembled via non-covalent bonding [3–6].

Hydrogen bonding is one of the key interactions for chemical and biological process in nature due to its stability, directionality, and dynamics. For molecular aggregates, hydrogen bonding plays an important role in the association of molecules. The first compounds found

to exhibit liquid crystalline behaviour due to hydrogen bond formation were carboxylic acids [7]. These compounds dimerize through intermolecular hydrogen bonds leading to a lengthening of the rigid-rod moiety, which in turn induces liquid crystallinity. Many liquid crystal systems containing hydrogen bonds that function between identical molecules have been reported [8–11].

A new type of thermotropic supramolecular liquid crystal obtained by molecular recognition processes through intermolecular hydrogen bonds were reported by Kato and Fréchet [12] and Lehn *et al.* [13]. The novelty of these works lie with the use of hetero-intermolecular bonds in order to assemble the mesogenic core, i.e. the two interacting molecules are not identical; such studies provide excellent examples of specific molecular recognition. After these findings, many liquid crystalline materials including low molar mass liquid crystals, main or side chain liquid crystalline polymers, and ferroelectric liquid crystals have been prepared using the intermolecular hydrogen bond [14–27].

Mixtures of unlike hydrogen-bonded molecules producing liquid crystals frequently involve donor molecules derived from benzoic acids with acceptor molecules derived from pyridine and 4,4′-bipyridine [14, 15]. As these systems had proved to be mesomorphic, we modified the benzoic acids to include an additional conjugated

*Author for correspondence; e-mail: wczin@postech.ac.kr

C=C bond, thus enhancing the structural anisotropy. It was reported that benzoic acids with $pK_a \sim 4$ can yield hydrogen-bonded complexes with pyridine derivatives [28]. The pK_a of benzoic acid is 4.19, while that of cinnamic acid is 4.44 at 25°C [29]; thus cinnamic acids, like benzoic acids, will be able to complex with various pyridine derivatives. This paper describes the phase behaviour of hydrogen-bonded liquid crystalline complexes of *n*-alkoxycinnamic acids with 4,4'-bipyridine. The result is compared with the mesophase formation of other hydrogen-bonded liquid crystalline complexes, described by others [14].

2. Experimental

4-*n*-Alkoxycinnamic acids (*n*CNA: $n = 4$–8, 10, 12, 16, 18, where *n* is the number of carbons in the alkoxy chain) were prepared according to known procedures [30, 31]. The compounds were recrystallized from ethanol and then from ethyl acetate; the transition temperatures agreed with published values [7 c]. *n*CNAs are mesomorphic materials due to their dimerization. 4,4'-Bipyridine (BPy) was purchased from Aldrich Chemical Co. and was sublimed before use. The complexes of *n*CNA with BP examined in the present study were prepared by the evaporation technique [32] from THF solution containing a 2 : 1 molar ratio of H-bond donor and acceptor moieties. The complex of *n*CNA with BPy is designated as *n*CNABPy.

Infrared (IR) spectra at various temperatures were obtained using a Shimadzu FTIR 4300 spectrophotometer. Sandwich cells were prepared by using a KBr pellet with an accessible optical range of 5000–400 cm^{-1}; the resolution was 4 cm^{-1}. The sample holder was heated by two cartridge heaters. A Perkin Elmer DSC-7 differential scanning calorimeter was used to determine the thermal transitions, with heating and cooling rates of 10°C min^{-1}. A volatile aluminum sample pan was used to minimize the evaporation of BPy in the isotropic state. The optical textures of the mesophases were studied with a Zeiss JENALAB-pol polarizing microscope (magnification: 160×) equipped with a Linkam LTS 350 hot stage and a TMS 93 temperature controller. X-ray diffractograms were obtained with synchrotron radiation at the 3C2 and 4C2 X-ray beam line ($\lambda = 0.1608$ nm) at the Pohang Accelerator Laboratory, Korea. *In-situ* X-ray measurements were performed in the transmission mode at various temperatures. The sample holder was heated with two cartridge heaters, and the temperature was monitored. A 7 μm thick Kapton film window was used to contain the samples in the fluid liquid crystalline states, and the scattered intensity from the Kapton window was subtracted.
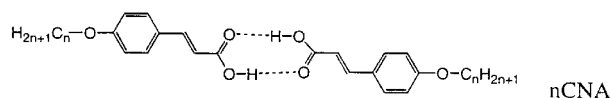
3. Results and discussion

3.1. *Thermal properties of nCNA compounds and the formation of nCNABPy complexes*

The thermal properties of *n*CNA compounds are given in figure 1. All of the *n*CNAs exhibit liquid crystalline behaviour due to dimerization of the alkoxycinnamic acid unit [7 c]. 4,4'-Bipyridine is non-mesomorphic, and melts directly to the isotropic liquid at 114°C.

The hydrogen-bonded mesogenic structure formed through complexation between H-bond donor and acceptor moieties designed for the present study is shown in figure 2. The technique used to form these complexes involves the dissolution of both components in THF, causing the breaking of existing H-bonds within *n*CNA dimers, followed by the slow evaporation of the THF, resulting in the self-assembly of the final complexes. Figure 2 displays the supramolecular structure of this complex.

The formation of H-bonded liquid crystal complexes, as shown in figure 2, was confirmed by IR spectroscopic experiments. The IR spectra showed the characteristic stretching bands (two bands centred around 2500 and 1900 cm^{-1}) resulting from self-association of carboxylic acid and pyridine through intermolecular hydrogen bonding [28]. Figure 3 shows the IR spectra of 12CNABPy in the range 3500–1500 cm^{-1} from room temperature to 190°C. The intensities of the bands at 2500 and 1900 cm^{-1} decreased with temperature increase, and then disappeared at the isotropic (I) phase; on cooling the isotropic phase these two bands reappeared. The reappearance of these bands demonstrates that H-bonding between *n*CNA and BPy is thermally reversible.

4CNA	Cr 154		N 185		I	
5CNA	Cr 140		N 177		I	
6CNA	Cr 147		N 177		I	
7CNA	Cr 144		N 173		I	
8CNA	Cr 141		N 172		I	
10CNA	Cr 131	S 150	N 169		I	
12CNA	Cr 127	S 156	N 164		I	
16CNA	Cr 123	S 158			I	
18CNA	Cr 122	S 155			I	

Figure 1. Thermal properties of *n*CNA compounds transition temperatures in °C.
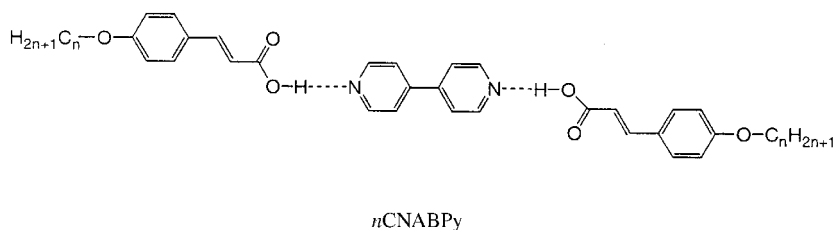
*n*CNABPy

Figure 2.   Hydrogen-bonded complexes of *n*CNAs with BPy.
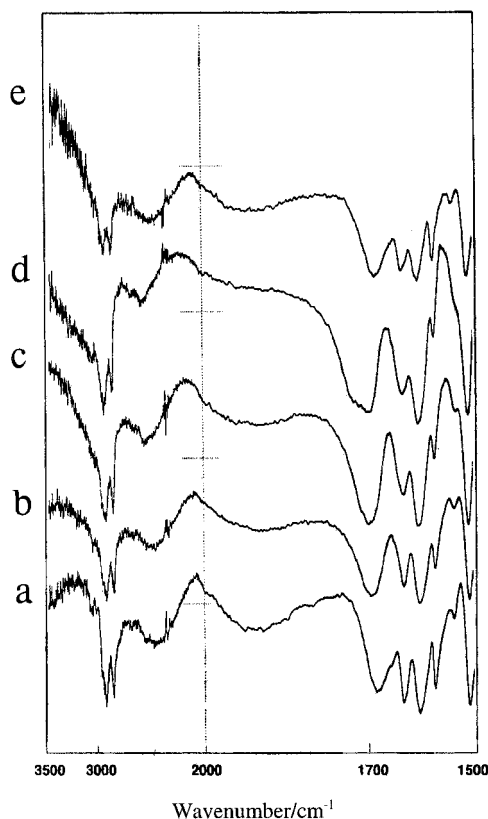
Figure 3.   Infrared spectra of 12CNABPy in the range 3500–1500 cm^{-1} at various temperatures: (*a*) room temperature, (*b*) 120°C, (*c*) 140°C, (*d*) 190°C, (*e*) room temperature (cooling).

3.2. *Mesomorphic properties of nCNABPy complexes*

*n*CNABPy complexes show enantiotropic liquid crystalline behaviour, as revealed by differential scanning calorimetry (DSC) and polarizing optical microscopy (POM). All the complexes behave similarly to the single mesogenic component and show clear phase transitions. The detailed phase behaviour of the complexes, however, is different from those of each of the H-bond donor and acceptor compounds. The thermal behaviour of the complexes confirms the selective formation of the H-bonded mesogen, as shown in figure 2. The phases and transition temperatures of these compounds are summarized in the table. The enthalpy changes of the nematic (N)–I transition for *n*CNABPy with *n* = 4–7 increase from 7.8 to 19.1 kJ mol^{-1}, and those of the smectic C (SmC)–I transition for *n*CNABPy with *n* = 10–18 increase from 27.5 to 32.7 kJ mol^{-1} with the increase in length of the alkoxy chain. However, the enthalpy changes of the SmC–smectic A (SmA) transitions for *n*CNABPy with *n* = 6–8 are too small to be observed in DSC thermograms; the transition temperature was therefore measured by XRD (see later). A general comparison of *n*CNABPy with the benzoic acid analogues, (*n*OBA)$_2$-BPy, shows that the transition temperatures of *n*CNABPy are generally higher than those of (*n*OBA)$_2$-BPy [14] because the mesogenic length of *n*CNABPy is longer than that of (*n*OBA)$_2$-BPy.

8CNA exhibits a nematic liquid crystalline phase. On cooling from the isotropic liquid, the droplet growth of

Table.   Thermal transitions of *n*CNABPy complexes: data obtained from the second heating scan. Temperatures in °C; enthalpies (in parentheses) in kJ mol^{-1}.

Complex	Phase transitions			
4CNABPy	Cr 150(41.8)	N 166(7.8)	I	
5CNABPy	Cr 137(30.0)	SmA 146(0.6)	N 162(9.4)	I
6CNABPy	Cr 132(30.0)	SmC 150[a](−)	SmA 158(2.0)	N 165(15.7) I
7CNABPy	Cr 128(33.3)	SmC 154[a](−)	SmA 159(−)	N 161(19.1)[b] I
8CNABPy	Cr 134(39.0)	SmC 162[a](−)	SmA 164(22.7)	I
10CNABPy	Cr 134(40.5)	SmC 165(27.5)	I	
12CNABPy	Cr 127(41.9)	SmC 162(27.9)	I	
16CNABPy	Cr 122(48.5)	SmC 160(32.7)	I	
18CNABPy	Cr 121(54.4)	SmC 157(32.7)	I	

[a] Measured using X-ray diffraction.
[b] Combined SmA–N–I transition.

(a)

(b)
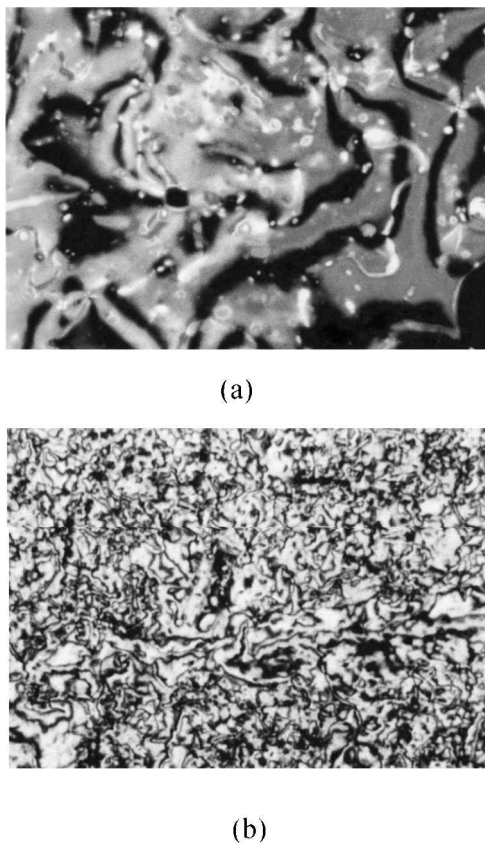
Figure 4.   Representative polarized optical micrographs ($160\times$) of the texture exhibited by (*a*) the nematic phase of 8CNA at 160°C on cooling, (*b*) the smectic C phase of 8CNABPy at 140°C on cooling.

texture can first be observed, with a final development of schlieren texture, characteristic of a nematic phase, figure 4(*a*) [33]. In contrast, the complexation of BPy to 8CNA induces the formation of smectic mesophases. Figure 4(*b*) is a blurred schlieren texture of 8CNABPy which is characteristic of a smectic C phase [33].

3.3. *X-ray studies of nCNABPy complexes*

To corroborate the molecular packing structure, the mesophases of *n*CNABPy were investigated by XRD. Figure 5 displays representative XRD patterns of 8CNABPy at various temperatures. Figure 5(*d*), obtained at room temperature, shows a number of sharp reflections in the wide angle region, indicating the crystalline nature of 8CNABPy at ambient temperature. On heating from its crystalline state, the sharp reflections of 8CNABPy disappeared and a diffuse halo was visible in the wide angle region, figure 5(*e*). Although there is a broad amorphous halo in the wide angle, the half-width Δq (scattering vector $q = 4\pi \sin \theta/\lambda$) of the wide angle halo increases from $3.0\,\text{nm}^{-1}$ (SmC) to $3.9\,\text{nm}^{-1}$ (I). This result may suggest that there is short range ordering of the mesogens in the smectic C liquid crystalline phase. Figure 5(*b*) exhibits the small angle XRD pattern at 140°C. The ratio of the positions of the two sharp peaks denotes that 8CNABPy exhibits a lamellar structure at its mesophase. 8CNABPy undergoes isotropization at 164°C as shown in figures 5(*c*) and 5(*f*). On cooling the isotropic phase, the smectic phase reappeared. The reappearance of the smectic morphology demonstrates
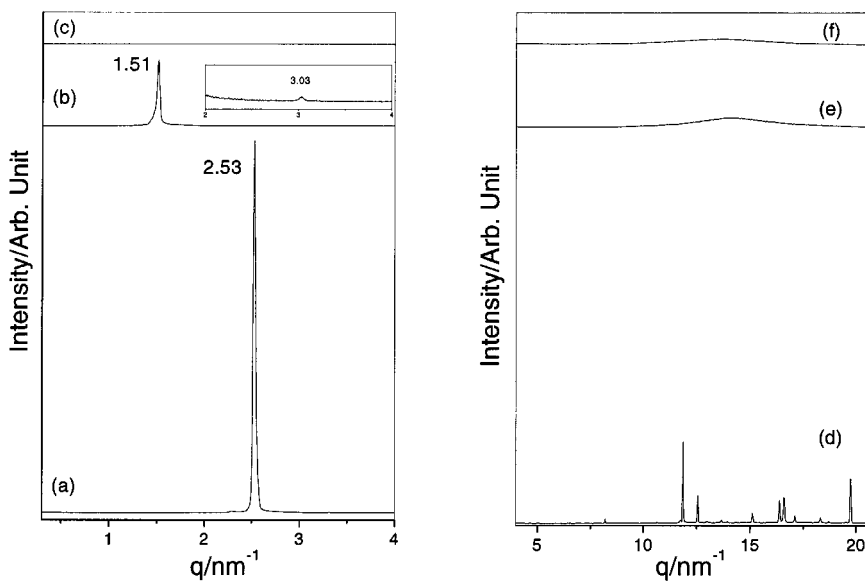

Figure 5.   X-ray diffractograms measured at different temperatures plotted against $q(= 4\pi \sin \theta/\lambda)$ for 8CNABPy. (*a*) Small angle and (*d*) wide angle XRD of the crystalline phase at room temperature; (*b*) small angle and (*e*) wide angle XRD of the smectic C phase at 150°C; (*c*) small angle and (*f*) wide angle XRD of the isotropic phase at 170°C.

that the transition is thermally reversible and hence that the phases of the H-bonded complex exist in equilibrium at a certain temperature region.

To investigate the smectic phase of *n*CNABPy complexes in more detail, X-ray measurement of the smectic layer spacing *d* of *n*CNABPy was made as a function of temperature. Representative plots of temperature-dependent layer spacings for *n*CNABPy are shown in figure 6. 6CNABPy and 8CNABPy display the increase in layer spacing as a function of increasing temperature, and its levelling-out at the transition. On the other hand, the layer spacing for 10CNABPy increases steadily with temperature. With increase of temperature, the tilt of the molecules with respect to the layer normal decreases, thus causing the increase in layer thickness for SmC phase. Thus the tilt angle of H-bonded complexes in the SmC phase is strongly temperature-dependent and decreases to zero at the phase transition to a smectic A phase like conventional calamitic (rod-like) mesogens [34]. In the smectic A phase, the layer spacing decreases slowly with increasing temperature, as shown in figure 6. So *n*CNABPy complexes have SmC and SmA phases in the range *n* = 6–8, whereas only the SmC phase occurs for *n* ⩾ 10. The existence of the SmA phase for *n*CNABPy with *n* = 5–7 could also be identified by POM. On heating, a dark texture was observed by POM between birefringent SmC and N textures. This isotropic texture under a homeotropic alignment indicates the optical uniaxial nature of the molecular arrangement in the SmA phase.

Figure 7 shows layer spacings as a function of the number of carbon atoms in the alkoxy chain, as measured in the smectic A phase. Since the molecules are aligned orthogonally to the layer in the SmA phase, the largest *d* spacing values of the SmA phase are
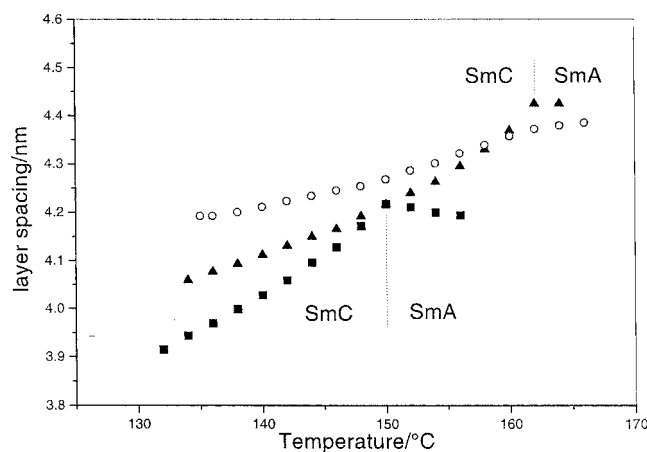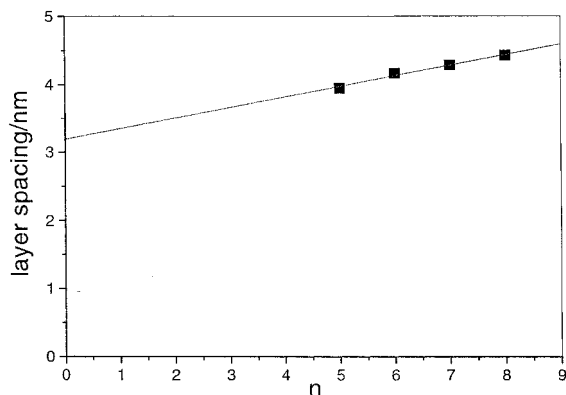

Figure 7. Layer spacing as a function of the number of carbon atoms in the alkoxy chain for 5–8CNABPy in the smectic A phase.

correlated to the length of the supramolecules. Thus the intercept value 3.19 nm can be ascribed to the length of the *n*CNABPy mesogenic moiety. The length of the mesogenic moiety for *n*CNABPy was calculated to be 3.08 nm when BPy lies between two cinnamic acid molecules, whereas the mesogenic length for the *n*CNA dimer is 1.96 nm. These results together with IR spectra confirm that BPy functions as a core unit in the liquid crystalline complex as shown in figure 2.

3.4. *Phase behaviour of nCNABPy complexes*

Figure 8(*a*) illustrates the phase behaviour for the *n*CNA series. As the chain length increases, smectic properties begin to appear, and as the range of smectic phase increases, the range of the nematic phase decreases with each successive chain increment, until in the hexadecyloxy and octadecyloxy compounds the smectic phase alone is found. For *n*CNABPy, the type of mesophase is also dependent on the length of the alkoxy chain. The variation of transition temperatures with the length of alkoxy chain is shown in figure 8(*b*). It is clear that increasing the alkoxy chain length on the cinnamic acid stabilizes the *n*CNABPy smectic phase. Only a nematic phase occurs for 4CNABPy; both smectic and nematic phases for *n*CNABPy with *n* = 5–7; and only smectic phases for the others.

A comparison of figures 8(*b*) and 8(*a*) shows that smectic phase is more common in the *n*CNABPy series. For example, the *n*CNA series show the nematic phase up to 8CNA, while the *n*CNABPy series display smectic phases from 5CNABP on. 8CNA shows a nematic phase between 142 and 172°C, whereas 8CNABPy displays smectic phases between 134 and 164°C. In 8CNABPy, the bipyridine unit is inserted between H-bonded 8CNA molecules, so the length of mesogen is increased. It is a somewhat striking result from the viewpoint of phase behaviour of rod-like mesogens, because most calamitic
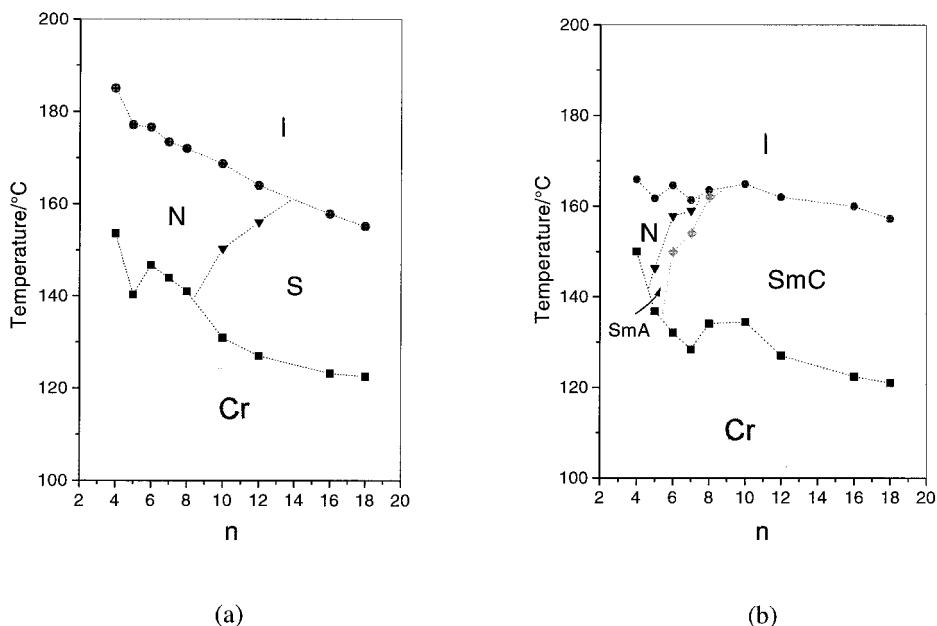

Figure 6. Temperature dependence of the layer spacing of 6CNABPy (solid square), 8CNABPy (solid triangle), and 10CNABPy (open circle).

(a)

(b)

Figure 8. Dependence of the transition temperature of (*a*) *n*CNA compounds and (*b*) *n*CNABPy complexes on the number of carbon atoms in the alkoxy chains.

liquid crystalline molecules stabilize the nematic phase with increasing rod volume fraction. Our speculation is that in 8CNABPy, insertion of BPy induces a much stronger H-bond than does the acid dimer, thus the polarity of the 8CNABPy mesogen must be larger than that of 8CNA. Thus, due to increased interaction energy density between polar rod and non-polar chain, the microphase-separated lamellar structure may be stabilized.

The phase behaviour of the *n*CNA and *n*CNABPy series displays a definite trend: as the length of the alkoxy chain increases, the smectic C phase is favoured. A similar trend was observed in the (*n*OBA)$_2$-BPy series [14]. These liquid crystalline molecules consist of two distinct and incompatible parts: an H-bonded rigid central unit and flexible and hydrophobic chains at both ends. The number of unfavourable contacts between hydrophobic, flexible chains and polar, rigid rods decreases when microphase-segregated assemblies are formed. According to the model suggested by Halperin [35], the aggregated rods are expected to favour ordered packing with their long axes aligned. In this structure, the rods are aligned and their tips toe the basal planes to achieve the minimum of surface free energy. When the melted chains grafted to the basal plane are long enough, the free energy induced by the chain elongation is so large that the rod tilts in order to increase the separation between grafting sites. As the alkoxy chain becomes longer, SmC phase is more favoured.

References

[1] WHITESIDES, G. M., MATHIAS, J. P., and SETO, C. T., 1991, *Science*, **254**, 1312.

[2] DEMUS, D., 1998, in *Handbook of Liquid Crystals*, Vol. 1, edited by D. Demus, J. Goodby, G. W. Gray, H.-W. Spiess, and V. Vill (Weinheim: Wiley-VCH), pp. 133–153.

[3] BRUCE, D. W., DUNMUR, D. A., LALINDE, E., MAITLIS, P. M., and STYRING, P., 1986, *Nature*, **323**, 791.

[4] RINGSDORF, H., WUSTEFELD, R., ZERTA, E., EBERT, M., and WENDORFF, J. H., 1989, *Angew. Chem. int. Ed. Engl.*, **28**, 914.

[5] PALEOS, C. M., and TSIOURVAS, D., 1995, *Angew. Chem. int. Ed. Engl.*, **43**, 1696.

[6] KATO, T., and FRECHET, J. M. J., 1995, *Macromol. Symp.*, **98**, 311.

[7] (*a*) BRADFIELD, E., and JONES, B., 1929, *J. chem. Soc.*, 2661; (*b*) BENNETT, G. M., and JONES, B., 1939, *J. chem. Soc.*, 420; (*c*) GRAY, G. W., and JONES, B., 1954, *J. chem. Soc.*, 1467.

[8] BEGINN, U., and LATTERMANN, G., 1994, *Mol. Cryst. liq. Cryst.*, **241**, 215.

[9] KLEPPINGER, R., LILLYA, P., and YANG, C., 1997, *J. Am. chem. Soc.*, **119**, 4097.

[10] SUAREZ, M., LEHN, J.-M., ZIMMERMAN, S. C., SKOULIOUS, A., and HEINRICH, B., 1998, *J. Am. chem. Soc.*, **120**, 9526.

[11] KANG, S. K., SAMULSKI, E. T., KANG, P., and CHOO, J., 2000, *Liq. Cryst.*, **3,** 377.

[12] KATO, T., and FRÈCHET, J. M. J., 1989, *J. Am. chem. Soc.*, **111,** 8533.

[13] BRIENNE, M.-J., GABARD, J., LEHN, J.-M., and STIBOR, I., 1989, *J. chem. Soc. chem. Commun.*, 1868.

[14] KATO, T., FRÈCHET, J. M. J., WILSON, P. G., SAITO, T., URYU, T., FUJISHIMA, A., JIN, C., and KANEUCHI, F., 1993, *Chem. Mater.*, **5,** 1094.

[15] GRUNERT, M., HOWIE, R. A., KAEDING, A., and IMIRE, C. T., 1997, *J. mater. Chem.*, **7,** 211.

[16] KATO, T., FUKUMASA, M., and FRÈCHET, J. M. J., 1995, *Chem. Mater.*, **7,** 368.

[17] BERNHARDT, H., WEISSFLOG, W., and KRESSE, H., 1996, *Angew. Chem. int. Ed. Engl.*, **35,** 874.

[18] (*a*) WILLIS, K., PRICE, D. J., ADAMS, H., UNGAR, G., and BRUCE, D. W., 1995, *J. mater. Chem.*, **5,** 2195; (*b*) FRIOT, B., BOYD, D., WILLIS, K., DONNIO, B., UNGAR, G., and BRUCE, D. W., 2000, *Liq. Cryst.*, **27,** 605.

[19] PFAADT, M., MOESSNER, G., PRESSNER, D., VALIYAVEETTIL, S., BOEFFEL, C., MULLEN, K., and SPIESS, H. W., 1995, *J. mater. Chem.*, **5,** 2265.

[20] TIAN, Y., XU, X., ZHAO, Y., TANG, X., and LI, T., 1997, *Liq. Cryst.*, **22,** 87.

[21] FOUQUEY, C., LEHN, J.-M., and LEVELUT, A.-M., 1990, *Adv. Mater.*, **2,** 254.

[22] ALEXANDER, C., JARIWALA, C. P., LEE, C. M., and GRIFFIN, A. C., 1994, *Macromol. Symp.*, **77,** 283.

[23] SINGH, A., LVOV, Y., and QADRI, S. B., 1999, *Chem. Mater.*, **11,** 3196.

[24] LEE, M., CHO, B.-K., KANG, Y.-S., and ZIN, W.-C., 1999, *Macromolecules*, **32,** 8531.

[25] (*a*) KATO, T., and FRÈCHET, J. M. J., 1989, *Macromolecules*, **22,** 3818; (*b*) KUMAR, U., KATO, T., and FRÈCHET, J. M. J., 1992, *J. Am. chem. Soc.*, **114,** 663; (*c*) KATO, T., KUBOTA, Y., URYU, T., and UJIIE, S., 1997, *Angew. Chem. int. Ed. Engl.*, **36,** 1617.

[26] RUOKOLAINEN, J., SAARIAHO, M., IKKALA, O., TEN BRINKE, G., THOMAS, E. L., TORKKELI, M., and SERIMAA, R., 1999, *Macromolecules*, **32,** 1152.

[27] (*a*) KUMAR, U., FRÈCHET, J. M. J., KATO, T., UJIIE, S., and TIMURA, K., 1992, *Angew. Chem. int. Ed. Engl.*, **31,** 1531; (*b*) KATO, T., KIHARA, H., URYU, T., UJIIE, S., IIMURA, K., FRÈCHET, J. M. J., and KUMAR, U., 1993, *Ferroelectrics*, **148,** 161; (*c*) KIHARA, H., KATO, T., URYU, T., UJIIE, S., KUMAR, U., FRÈCHET, J. M. J., BRUCE, D. W., and PRICE, D. J., 1996, *Liq. Cryst.*, **21,** 25.

[28] JOHNSON, S. L., and RUMON, K. A., 1965, *J. phys. Chem.*, **69,** 74.

[29] WEAST, R. C., 1988, in *CRC Handbook of Chemistry and Physics* (CRC Press), D-101.

[30] GARANTI, L., SALA, A., and ZECCHI, G., 1975, *J. org. Chem.*, **40,** 2403.

[31] FURNISS, B. S., HANNAFORD, A. J., SMITH, P. W. G., and TATCHELL, A. R., 1989, in *Vogel's Textbook of Practical Organic Chemistry*, 5th Edn (Longman Scientific & Technical), p. 1041.

[32] DE MEFTAHI, M. V., and FRÈCHET, J. M. J., 1988, *Polymer*, **29,** 477.

[33] DEMUS, D., and RICHTER, L., 1978, in *Textures of Liquid Crystals* (Verlag Chemie), pp. 106–211.

[34] SEDDON, J. M., 1998, in *Handbook of Liquid Crystals*, Vol. 1, edited by D. Demus, J. Goodby, G. W. Gray, H.-W. Spiess, and V. Vill (Weinheim: Wiley-VCH), pp. 635–640.

[35] HALPERIN, A., 1990, *Macromolecules*, **23,** 2724.